Proceedings of the 42nd IEEE
Conference on Decision and Control
Maui, Hawaii USA, December 2003

Event-based PI Control of an Underactuated Biped Walker

J.W. Grizzle
EECS Department
University of Michigan
Ann Arbor, Michigan 48109-2122, USA
E-mail: grizzle@umich.edu

E.R. Westervelt
Department of Mechanical Engineering
The Ohio State University
Columbus, Ohio 43210-1154, USA
E-mail: westervelt.4@osu.edu

C. Canudas-de-Wit
Laboratoire d'Automatique de Grenoble
INPG-ENSIEG
BP 46, Saint-Martin-d'Hères, Cedex, France
E-mail: canudas@lag.ensieg.inpg.fr

Abstract— **This paper addresses the control of a planar, biped robot with one degree of underactuation. Previous work has designed controllers that induce provably, exponentially stable, periodic walking motions at fixed, pre-determined walking rates. These controllers operate in continuous time during the single support phase of the robot. The present paper shows how to design an event-based PI controller that provides an additional control feature: the ability to regulate the average walking rate to a continuum of values. The PI controller is active only in the (instantaneous) double support phase and achieves regulation by adjusting key parameters of the within-stride controller.**

I. Introduction

The robots treated in this paper consist of N-links connected in a planar tree structure to form at least two identical legs, with the legs connected at a common point called the hips. All links have mass, are rigid, and are connected in revolute joints (see Fig. 1(a)). Furthermore, no actuation is applied between the stance leg and the ground, while all other joints are actuated. A rigid impact is used to model the contact of the swing leg with the ground.

Addressing the control of robots without actuation between the stance leg and ground is an important step in designing natural and efficient walking motions. To date, the control of robots with feet has been based on the zero moment point (ZMP) principle [4] which explicitly seeks to avoid the underactuation that occurs when the stance foot naturally roles up on the toe prior to heel strike by the swing leg. In a robot without feet, the ZMP heuristic is not applicable, and thus underactuation must be explicitly addressed in the feedback control design, leading to the development of new feedback stabilization methods. Moreover, it is anticipated that these results will lead to a control theory for walking with feet that will allow anthropomorphic foot action.

This paper builds on the results in [11] and [10]. The notion of the hybrid zero dynamics for the walking motion of a class of planar biped robots with point feet was treated in [11]. The hybrid zero dynamics is a two-dimensional, invariant sub-dynamics of the complete hybrid model of the biped robot. It was shown to be key to designing exponentially stabilizing controllers for walking motions. In particular, exponentially stable orbits of the hybrid zero dynamics can be rendered exponentially stable in the complete hybrid model. The Poincaré map of the hybrid zero dynamics was proven to be diffeomorphic to a scalar, LTI system, rendering transparent the existence and stability properties of periodic orbits of the hybrid zero dynamics. A special class of output functions based on Bézier polynomials was used to simplify the computation of the hybrid zero dynamics, while at the same time inducing a convenient, finite parameterization of these dynamics. Parameter optimization was then applied to the hybrid zero dynamics to directly design a stable, closed-loop system that satisfied design constraints, such as walking at a given average walking rate and the forces on the support leg lying in the allowed friction cone. Stability of the closed-loop system was established with a Poincaré analysis and not by appealing to heuristics, such as the ZMP. All of the results were illustrated on a five-link walker (see Fig. 1(b)).

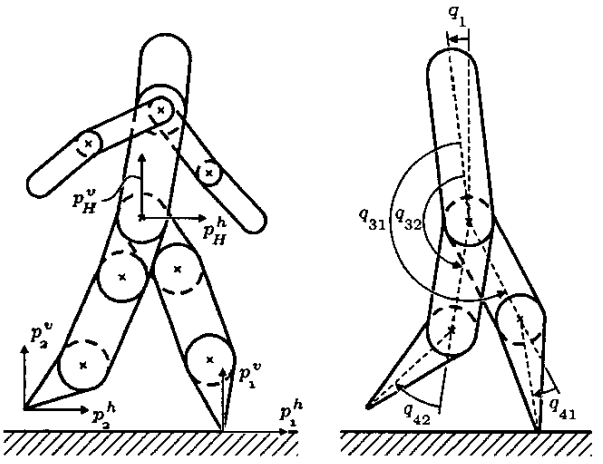

(a) A representative example of the class of -link biped robot models considered. Cartesian coordinates are indicated at the hips and the leg ends.

(b) Schematic of the example 5-link biped considered with measurement conventions.

Fig. 1. Example bipeds. No actuation is applied between the stance leg and the ground, while all other joints are actuated; the two legs are symmetric. In single support, the stance leg is assumed to be at the origin of the world coordinate frame. Consequently, at impact, $\frac{h}{2}$ measures step length.

0-7803-7924-1/03/$17.00 ©2003 IEEE

The present paper provides an additional feature: the ability to regulate the robot's average walking rate to a continuum of values via event-based PI control. The PI controller is active only in the (instantaneous) double support phase and achieves regulation by adjusting key parameters of the in-stride controller. A special case of the results presented here has appeared in [10]. In particular, [10] assumed that the parameters used for event-based control affected the linearization of the restricted Poincaré map of the hybrid zero dynamics but did not directly affect the linearization of the function that computes average walking rate. The more general case of when the parameters used for event-based control affect both quantities in a non-trivial way is addressed here. In addition, considerably more detail concerning the stability proof of the controller is provided in this communication.

Section II summarizes some pertinent notation and results from [11]. Section III develops an event-based PI controller to regulate walking rate to a continuum of values. The controller uses integral action to adjust the parameters in a controller that, for fixed parameter values, induces an exponentially stable, periodic orbit. Parameter adjustment takes place just after impact (swing leg touching the ground). The analysis and design of the controller are based on the restricted Poincaré map of the hybrid zero dynamics.

Section IV illustrates the application of the event-based PI controller of Section III on the five-link biped model studied in [3], [8], [9], [11] (see Fig. 1(b)). Here, simulation will be used to demonstrate the controller's performance under a variety of errors between the control design model and the actual model. Robustness to disturbances is illustrated by application of an external force acting on the hips. Robustness to parameter mismatch is demonstrated through variation of masses and inertias. Robustness to structural mismatch is illustrated by walking on a *compliant walking surface* [8]. Animations of the resulting walking motions are available at [5]. Experiments employing event-based PI control have been conducted on RABBIT [1] and will be reported elsewhere; see [5] for videos and further information.

II. Notation and Basic Facts

This section summarizes some notation and results from [11] that are used extensively in this communication. The reader is encouraged to read [11] for further interpretation, context and supporting diagrams, and [2] for a less technical overview of the control design methodology.

The configuration coordinates of the robot in single support (also commonly called the swing phase) are denoted by $q = (q_1, \cdots, q_N)' \in \mathcal{Q}$, the state space is denoted by $T\mathcal{Q}$, and a control is applied at each connection of two links, but not at the contact point with the ground (i.e., no ankle torque), for a total of $(N-1)$ controls. The detailed assumptions on the robot (bipedal, planar and one less degree of actuation than degrees of freedom, point feet, rigid contact model) and the walking gait (instantaneous double support phase, no slipping nor rebound at impact, motion from left to right, symmetric gait) are given in [11, Sec. II].

The hybrid model of the robot (single support phase Lagrangian dynamics plus impact map) is expressed as a nonlinear system with impulse effects

$$\begin{array}{rcll} \dot{x} & = & f(x) + g(x)u & x^- \notin S \\ x^+ & = & \Delta(x^-) & x^- \in S. \end{array} \tag{1}$$

The impact or walking surface, S, is defined as

$$S := \{(q, \dot{q}) \in T\mathcal{Q} \mid p_2^v(q) = 0,\ p_2^h(q) > 0\}, \tag{2}$$

where p_2^v and p_2^h are the Cartesian coordinates of the swing leg end (see Fig. 1(a)). The impact map $\Delta : S \to TQ$ computes the value of the state just after impact with S, $x^+ = (q^+, \dot{q}^+)$, from the value of the state just before impact, $x^- = (q^-, \dot{q}^-)$. Since the configuration coordinates necessarily involve the specification of which of the two the legs is in contact with the ground, the coordinates must be relabeled after each step to take into account the successive changing of the support leg. This is reflected in the impact map via a constant, invertible matrix R, $q^+ := Rq^-$.

The control design involves the choice of a set of holonomic constraints that are asymptotically imposed on the robot via feedback control. This is accomplished by interpreting the constraints as output functions depending only on the configuration variables of the robot, and then combining ideas from finite-time stabilization and computed torque. The outputs $y \in \mathbb{R}^{N-1}$ are chosen as

$$y = h(q, \alpha) = H_0 q - h_d(\theta(q), \alpha), \tag{3}$$

with terms defined as follows.

1) H_0 is an $(N-1) \times N$ matrix of real coefficients specifying what is to be controlled.
2) $\theta(q) := cq$, where c is a $1 \times N$ row vector of real coefficients, is a scalar function of the configuration variables and should be chosen so that it is monotonically increasing along a step of the robot ($\theta(q)$ is playing the role of time). Define $\theta^+ = cq^+$ and $\theta^- = cq^-$ to be the initial and final values of θ, respectively, along a step.
3) Normalization of θ to take values between zero and one,
$$s(q) := \frac{\theta(q) - \theta^+}{\theta^- - \theta^+}. \tag{4}$$
4) Bézier polynomials of order $M \geq 3$
$$b_i(s) := \sum_{k=0}^{M} \alpha_k^i \frac{M!}{k!(M-k)!} s^k (1-s)^{M-k}. \tag{5}$$
5) For α_k^i as above, define the $(N-1) \times 1$ column vector $\alpha_k := (\alpha_k^1, \cdots, \alpha_k^{N-1})'$ and the $(N-1) \times (M+1)$ matrix $\alpha := [\alpha_0, \cdots, \alpha_M]$.
6)
$$h_d(\theta(q), \alpha) := \begin{bmatrix} b_1 \circ s(q) \\ \vdots \\ b_{N-1} \circ s(q) \end{bmatrix}. \tag{6}$$

The matrix of parameters α is said to be a regular parameter of output (3) if the output satisfies [11, Sec. III.A, HH1–HH4] and [11, Sec. III.B, HH5], which together imply the

invertibility of the decoupling matrix and the existence of a two-dimensional, smooth, zero dynamics associated with the single support phase of the robot. Let Z_α be the (swing phase) zero dynamics manifold. Let Γ_α be any feedback satisfying [11, Sec. III.C, CH2–CH5] so that Z_α is invariant under the swing phase dynamics in closed loop with Γ_α and is locally finite-time attractive otherwise. Note that standard results imply that $\Gamma_\alpha|_{Z_\alpha} = -(L_g L_f h)^{-1} L_f^2 h$ [7], and thus (i) $\Gamma_\alpha|_{Z_\alpha}$ is uniquely determined by the choice of parameters used in the output and is completely independent of the choice of feedback used to drive the constraints to zero in finite time; and (ii) even though Γ_α is necessarily not smooth, $\Gamma_\alpha|_{Z_\alpha}$ is as smooth as the robot model.

For a regular parameter value α of output (3), the definition of the outputs and basic properties of Bézier polynomials yield a very simple characterization of $S \cap Z_\alpha$, the configuration and velocity of the robot at the end of a phase of single support. Define

$$q_\alpha^- = H^{-1} \begin{bmatrix} \alpha_M \\ \theta_\alpha^- \end{bmatrix} \tag{7}$$

$$\omega_\alpha^- = H^{-1} \begin{bmatrix} \dfrac{M}{\theta_\alpha^- - \theta_\alpha^+} (\alpha_M - \alpha_{M-1}) \\ 1 \end{bmatrix}, \tag{8}$$

where $H := [H_0' \ c]'$, and the initial and final values of θ corresponding to this output are denoted by θ_α^+ and θ_α^-, respectively. Then $S \cap Z_\alpha = \{(q_\alpha^-, \dot{q}_\alpha^-) \mid \dot{q}_\alpha^- = a\omega_\alpha^-, a \in \mathbb{R}\}$ and is determined by the *last two columns* of the parameter matrix α. In a similar fashion $\Delta(S \cap Z_\alpha)$, the configuration, q_α^+, and velocity, $\dot{q}_\alpha^+$, of the robot at the beginning of a subsequent phase of single support, may be simply characterized and are determined by the *first two columns* of the parameter matrix α. By [11, Th. 4] it follows that

$$\begin{bmatrix} \alpha_0 \\ \theta_\alpha^+ \end{bmatrix} = HRH^{-1} \begin{bmatrix} \alpha_M \\ \theta_\alpha^- \end{bmatrix} \tag{9}$$

implies $h(\cdot, \alpha) \circ \Delta|_{(S \cap Z_\alpha)} = 0$, while, if $\dot{q}_\alpha^+ := \Delta_{\dot{q}}(q_\alpha^-)\omega_\alpha^-$, results in $c\dot{q}_\alpha^+ \neq 0$, then

$$\alpha_1 = \frac{\theta_\alpha^- - \theta_\alpha^+}{Mc\dot{q}_\alpha^+} H_0 \dot{q}_\alpha^+ + \alpha_0 \tag{10}$$

implies $L_f h(\cdot, \alpha) \circ \Delta|_{(S \cap Z_\alpha)} = 0$. The key thing to note is that these two conditions involve, once again, only the *first two columns* of the parameter matrix α. In a similar fashion the *last two columns* of the parameter matrix α may be chosen so that $h(\cdot, \alpha)|_{(S \cap Z_\alpha)} = 0$, and $L_f h(\cdot, \alpha)|_{(S \cap Z_\alpha)} = 0$.

Conditions (9) and (10) imply that $\Delta(S \cap Z_\alpha) \subset Z_\alpha$, in which case Z_α is then controlled-invariant for the full hybrid model of the robot. The resulting restriction dynamics is called the *hybrid zero dynamics*. Necessary and sufficient conditions can be given for the hybrid zero dynamics to admit an exponentially[1] stable, periodic orbit, $\mathcal{O}_\alpha$, [11]. When these conditions are met, the matrix of parameters α is said to give rise to an exponentially stable walking motion. Under controller Γ_α, the exponentially stable orbit in the hybrid zero dynamics is also exponentially stable in the full order model, (1). The domain of attraction of $\mathcal{O}_\alpha$ in the full dimensional model cannot be easily estimated; however, its domain of attraction intersected with $S \cap Z_\alpha$, that is, the domain of attraction of the associated fixed-point of the restricted Poincaré map, $\rho_\alpha : S \cap Z_\alpha \to S \cap Z_\alpha$, is computed analytically in [11, Sec. IV].

III. Event-Based PI Control of the Average Walking Rate

The goal of this section is to design an event-based controller[2] that adjusts the parameters in the output (3) to achieve walking at a *continuum* of rates. The controller design and analysis are based on the hybrid zero dynamics. A one-parameter curve will be defined in the set of parameters appearing in (3). Conditions will be identified so that this one-parameter curve will yield an effective control for the associated Poincaré map. Updating this control at each impact event of the walking cycle will yield a means to control average walking rate.

Define the average walking rate over a step[3] to be step length (m) divided by the elapsed time of a step (s). For a given controller Γ_α satisfying the hypotheses of Section II, the average walking rate is computed from the model (1) as follows. Let $P_\alpha : S \to S$ be the Poincaré return map[4] and let $T_{I,\alpha} : TQ \to \mathbb{R}_{\geq 0} \cup \{\infty\}$ be the time to impact function. The average walking rate is formally defined as a (partial) map $\bar{\nu}_\alpha : S \to \mathbb{R}_{\geq 0}$ by

$$\bar{\nu}_\alpha := \frac{p_2^h \circ P_\alpha}{T_{I,\alpha} \circ \Delta}, \tag{11}$$

where, p_2^h, when evaluated on S, computes step length (see Fig. 1(a)). On the open subset $\tilde{S} \subset S$ where $0 < T_{I,\alpha} \circ \Delta < \infty$ and the associated impacts are transversal to S, both P_α and $T_{I,\alpha} \circ \Delta$ are well-defined and continuous (see [6, Sec. III.B]). It follows that $\bar{\nu}_\alpha$ restricted to $\tilde{S}$ is continuous. Since Γ_α is continuous but not Lipschitz continuous, $\bar{\nu}_\alpha$ is not smooth on any open subset of S. However, if α is a regular parameter value of output (3) giving rise to a hybrid zero dynamics, $\Delta(S \cap Z_\alpha) \subset Z_\alpha$, then $\bar{\nu}_\alpha$ restricted to $\tilde{S} \cap Z_\alpha$ depends smoothly on the states and the parameter values α used to define the outputs, (3).

Let α be a regular parameter value of output (3) for which there exists a exponentially stable periodic orbit. Let z_α^* be the corresponding fixed point of the restricted Poincaré map, $\rho_\alpha : S \cap Z_\alpha \to S \cap Z_\alpha$. To emphasize the dependence on the parameter value, for $z \in S \cap Z_\alpha$, let $\rho(z, \alpha) := \rho_\alpha(z)$; similarly, $\bar{\nu}(z, \alpha) := \bar{\nu}_\alpha(z)$.

[1]Note that finite-time stabilization is used only to constrain (-1) of the degrees of freedom while the stability properties of the unactuated degree of freedom is determined by the hybrid zero dynamics.

[2]That is, one that acts step-to-step with updates occurring at impacts.

[3]A step starts with the swing leg on the ground and behind the robot and ends with the swing leg on the ground and in front of the robot.

[4]In general it is a partial map because not every point in results in a solution of the model that has an impact with .

Suppose that $\delta\alpha \in \mathbb{R}^{(N-1)\times(M+1)}$ is such that $\delta\alpha \neq 0$ and

$$(\delta\alpha)_0 = (\delta\alpha)_1 = (\delta\alpha)_{M-1} = (\delta\alpha)_M = 0. \tag{12}$$

Then, for $w \in \mathbb{R}$ sufficiently small in magnitude, $\alpha + w\delta\alpha$ is also regular. From (12)

$$\begin{array}{rcl} S \cap Z_{\alpha+w\delta\alpha} & = & S \cap Z_\alpha \\ \Delta(S \cap Z_{\alpha+w\delta\alpha}) & = & \Delta(S \cap Z_\alpha). \end{array} \tag{13}$$

Thus, $\rho_{\alpha+w\delta\alpha} : S \cap Z_\alpha \to S \cap Z_\alpha$, and the following single-input, single-output dynamic system can be defined,

$$\begin{array}{rcl} z(k+1) & = & \rho(z(k), \alpha + w(k)\delta\alpha) \\ \eta(k+1) & = & \bar{\nu}(z(k), \alpha + w(k)\delta\alpha) \\ y(k) & = & \eta(k), \end{array} \tag{14}$$

with two-dimensional state space $S \cap Z_\alpha \times \mathbb{R}$, input $w \in \mathbb{R}$ and output equal to average walking rate, $y \in \mathbb{R}$. It's linearization is

$$\begin{array}{rcl} \delta z(k+1) & = & a_{11}\delta z(k) + b_1 \delta w(k) \\ \delta\eta(k+1) & = & a_{21}\delta z(k) + b_2 \delta w(k) \\ \delta y(k) & = & \delta\eta(k), \end{array} \tag{15}$$

where[5]

$$\begin{array}{rcl} a_{11} & := & \dfrac{\partial \rho}{\partial z}(z, \alpha + w\delta\alpha)\Big|_{\substack{z=z^*_\alpha \\ w=0}} \\ b_1 & := & \dfrac{\partial \rho}{\partial w}(z, \alpha + w\delta\alpha)\Big|_{\substack{z=z^*_\alpha \\ w=0}} \\ a_{21} & := & \dfrac{\partial \bar{\nu}}{\partial z}(z, \alpha + w\delta\alpha)\Big|_{\substack{z=z^*_\alpha \\ w=0}} \\ b_2 & := & \dfrac{\partial \bar{\nu}}{\partial w}(z, \alpha + w\delta\alpha)\Big|_{\substack{z=z^*_\alpha \\ w=0}}. \end{array} \tag{16}$$

The linearized system (15) is clearly exponentially stable if, and only if, $|a_{11}| < 1$. An easy computation shows that its DC-gain is non-zero if, and only if,

$$a_{21}b_1 + b_2(1 - a_{11}) \neq 0. \tag{17}$$

Theorem 1: (Event-based PI control applied to the hybrid zero dynamics) Let α be a regular parameter value for which there exists an exponentially stable periodic orbit in Z_α. Denote the corresponding fixed point of the Poincaré return map by z^*_α. Assume there exists $\delta\alpha$ satisfying (12) and such that the non-zero DC-gain condition, (17), holds. Then average walking rate can be regulated via PI control. In particular, there exist $\epsilon > 0$, and scalars K_p and K_I such that for all η^* such that $|\eta^* - \bar{\nu}(z^*_\alpha)| < \epsilon$, the system consisting of (14) in closed loop with the proportional plus integral controller

$$\begin{array}{rcl} e(k+1) & = & e(k) + (\eta^* - \eta(k)) \\ w(k) & = & K_p(\eta^* - \eta(k)) + K_I e(k) \end{array} \tag{18}$$

has an exponentially stable equilibrium, and thus, when initialized sufficiently near the equilibrium, $\lim_{k\to\infty}(\eta^* - \eta(k)) = 0$. □

[5]We have abused notation and not made the distinction between as a point in that lies in $\cap$ $_\alpha$ and as a coordinate on $\cap$ $_\alpha$.

Proof: The linear system (15) is exponentially stable because the exponential stability of the fixed-point z^*_α implies that $|a_{11}| < 1$. This, combined with the DC-gain being non-zero, implies the existence of a PI controller of the form

$$\begin{array}{rcl} \delta e(k+1) & = & \delta e(k) + (\delta\eta^* - \delta\eta(k)) \\ \delta w(k) & = & K_p(\delta\eta^* - \delta\eta(k)) + K_I \delta e(k) \end{array} \tag{19}$$

such that the closed-loop system (15) with (19) is exponentially stable and satisfies $\lim_{k\to\infty}(\delta\eta^* - \delta\eta(k)) = 0$, where $\delta\eta^* := \eta^* - \bar{\nu}(z^*_\alpha, \alpha)$. Since the closed loop of (15) with (19) is the linearization of (14) in closed loop with (18), the result follows. ■

The PI controller in (18) is realized on the full-hybrid model of the robot as

$$\left.\begin{array}{rcl} \dot{x} & = & f(x) + g(x)\Gamma_{\alpha+w\delta\alpha} \\ \dot{e} & = & 0 \\ \dot{w} & = & 0 \\ \dot{\eta} & = & 0 \end{array}\right\} \quad x^- \notin S$$

$$\left.\begin{array}{rcl} x^+ & = & \Delta(x^-) \\ e^+ & = & e^- + (\eta^* - \eta^-) \\ w^+ & = & K_p(\eta^* - \eta^-) + K_I e^- \\ \eta^+ & = & \bar{\nu}(x^-, \alpha + w^+\delta\alpha) \end{array}\right\} \quad x^- \in S \tag{20}$$

where the extra states are used to store past values of $\bar{\nu}$ and w, and to implement the difference equation in the PI controller. The existence of an asymptotically stable orbit is analyzed next.

Theorem 2: (Event-based PI control applied to the full model) Assume the hypotheses of Theorem 1 and let Γ_α be any feedback satisfying [11, Sec. IV.C, CH2–CH5] (see also, [6, Sec. IV.B, CH2–CH5]) so that Z_α is invariant under the swing phase dynamics in closed loop with Γ_α and is locally finite-time attractive otherwise. Assume that K_p and K_I have been chosen so that (14) in closed loop with (18) has an exponentially stable equilibrium. Then the hybrid model (20) possesses an asymptotically stable orbit and $\lim_{t\to\infty}(\eta^* - \eta(t)) = 0$. □

Proof: By the proof of [6, Th. 2], it is enough to check that the restricted Poincaré map of (20) has an asymptotically stable fixed point. An easy computation gives that (14) in closed loop with (18) realizes the restricted Poincaré map, and thus the result follows. ■

Remark 1: Theorems 1 and 2 of [6] only addresses asymptotic stability of orbits. However, under the assumptions of Theorem 2 of [6], exponential stability can be shown. The key point is that $d \circ \Delta$ in [6, Eqn. (55)] is differentiable on $\tilde{S} \cap Z$, and hence is Lipschitz continuous. Since $d \circ \Delta$ vanishes at a fixed point of the restricted Poincaré map, say z^*, it follows that for a given coordinate chart on $\tilde{S} \cap Z$ there exists $L < \infty$ such that $d \circ \Delta(z) \leq L||z - z^*||$, and thus by [6, Eqn. (55)], exponential stability of the fixed point of the restricted Poincaré map implies the exponential stability of the orbit in the full state space. Since the converse is clear, it follows that under the assumptions of [6, Thm. 2], exponential stability of the fixed point of the restricted Poincaré map is equivalent to the exponential stability of the orbit in the full state space. △

Remark 2: An alternative realization of (20) can be given. Since from (12) the step length is fixed for all values of w, the average walking rate can be computed directly from its definition: step length divided by elapsed time for a step. This leads to

$$\left.\begin{array}{rcl}\dot{x} &=& f(x)+g(x)\Gamma_{\alpha+w\delta\alpha}\\ \dot{t} &=& 1\\ \dot{e} &=& 0\\ \dot{w} &=& 0\end{array}\right\} \quad x^- \notin S$$
$$\left.\begin{array}{rcl}x^+ &=& \Delta(x^-)\\ t^+ &=& 0\\ e^+ &=& e^- + (\eta^* - \frac{p_2^h(q_\alpha^-)}{t^-})\\ w^+ &=& K_p(\eta^* - \frac{p_2^h(q_\alpha^-)}{t^-}) + K_I e^-\end{array}\right\} \quad x^- \in S \qquad (21)$$

where $p_2^h(q_\alpha^-)$ computes step length; this is what is done in the simulations. △

Remark 3: Exponential stability of the nominal orbit gives $|a_{11}| < 1$, which implies that $1 - a_{11} > 0$. From [11, Eqns (81) and (85)], $a_{21} > 0$. Hence, a sufficient condition for the DC-gain (17) to be non-zero is $b_1 > 0$ and $b_2 > 0$. Thus, PI control of average walking speed is possible if one can find $\delta\alpha$ satisfying (12) and

$$\begin{aligned}\sum_{i=1}^{N-1}\sum_{k=2}^{M-2}\delta\alpha_k^i\frac{\partial\rho(z,\alpha)}{\partial\alpha_k^i}\bigg|_{z_\alpha^*} &> 0\\ \sum_{i=1}^{N-1}\sum_{k=2}^{M-2}\delta\alpha_k^i\frac{\partial\bar{\nu}(z,\alpha)}{\partial\alpha_k^i}\bigg|_{z_\alpha^*} &> 0.\end{aligned} \qquad (22)$$

Therefore, it is enough to find one pair of indices (k,i), with $2 \le k \le M-2$, and $1 \le i \le N-1$, such that

$$\frac{\partial\rho(z,\alpha)}{\partial\alpha_k^i}\bigg|_{z_\alpha^*} \quad \text{and} \quad \frac{\partial\bar{\nu}(z,\alpha)}{\partial\alpha_k^i}\bigg|_{z_\alpha^*} \qquad (23)$$

are both non-zero and have the same sign. This condition will be verified on the example. △

Remark 4: The relation to the result in [10, Sec. IV] is established as follows. Suppose that there exist two pairs of indices (k_j, i_j), $2 \le k_j \le M-2$, and $1 \le i_j \le N-1$, $j = 1,2$, such that

$$\begin{vmatrix} \frac{\partial\rho(z,\alpha)}{\partial\alpha_{k_1}^{i_1}}\Big|_{z_\alpha^*} & \frac{\partial\rho(z,\alpha)}{\partial\alpha_{k_2}^{i_2}}\Big|_{z_\alpha^*} \\ \frac{\partial\bar{\nu}(z,\alpha)}{\partial\alpha_{k_1}^{i_1}}\Big|_{z_\alpha^*} & \frac{\partial\bar{\nu}(z,\alpha)}{\partial\alpha_{k_2}^{i_2}}\Big|_{z_\alpha^*}\end{vmatrix} \neq 0. \qquad (24)$$

Then there exists $\delta\alpha$ satisfying (12) and

$$\begin{aligned}\sum_{i=1}^{N-1}\sum_{k=2}^{M-2}\delta\alpha_k^i\frac{\partial\rho(z,\alpha)}{\partial\alpha_k^i}\bigg|_{z_\alpha^*} &> 0\\ \sum_{i=1}^{N-1}\sum_{k=2}^{M-2}\delta\alpha_k^i\frac{\partial\bar{\nu}(z,\alpha)}{\partial\alpha_k^i}\bigg|_{z_\alpha^*} &= 0;\end{aligned} \qquad (25)$$

for which b_2 in (16) is then equal to zero. In this case, (17) reduces to $a_{21}b_1 \neq 0$, which is equivalent to the condition given in [10, Eqn (16)]. △

Remark 5: What if the nominal orbit is not exponentially stable (i.e., $|a_{11}| \ge 1$)? If (15) is stabilizable, then the non-zero DC-gain condition (17) is equivalent to stabilizability of (15) augmented with the integrator of (19). Exponentially stable regulation can be achieved therefore with a slight extension to the PI controller:

$$\begin{aligned}e(k+1) &= e(k) + (\eta^* - \eta(k)) \qquad (26)\\ w(k) &= K_p(\eta^* - \eta(k)) + K_I e(k) + K_3(z(k) - z^*(k))\end{aligned}$$
△

IV. Illustration of the Result

This section illustrates how the presented technique affords the construction of a feedback controller that induces walking at a continuum of rates while providing stabilization and a modest amount of robustness to disturbances, to parameter mismatch between the design model and the actual robot, and to structural mismatch between the design model and the actual robot. The results are illustrated via three simulations on the five-link model (see Fig. 1(b)) studied in [3], [8], [9], [11]. For reasons of space, the details of the model are omitted and the reader is referred to [11]. Animations of the three examples as well as additional supporting plots may be found at [5].

For the following three examples finite differences were used to verify the sufficient condition shown in (22) for several values of i and k. In this way, it was determined that adjusting the angle of the swing leg femur during mid-step would have a sufficiently strong effect on the average walking speed (this corresponded to $i = 2$ and $k = 3$). Hence, $\delta\alpha$ was chosen to be all zeros with the exception of $\delta\alpha_3^2$ which was set to 1.

A. Robustness to disturbances

This example will illustrate robustness to disturbances by simulation of the robot with an external force acting on the hips. Event-based PI control is used to reject a 3 N external force acting horizontally at the robot's hip opposite to the direction of walking.

The robot is initialized at the fixed point of a controller with average walking rate equal to 0.50 m/s. Event-based PI control with gains $K_p = 5$ and $K_I = 2$ and set-point $\eta^* = 0.5$ is applied starting on the second step coincident with the application of a constant 3 N force acting at the hips. Fig. 2(a) depicts the actual walking rate versus the commanded value of 0.50 m/s. The peak torque for this example is 70.1 Nm, about half of the 150 Nm that is possible with the motors and gearing of the robot studied in [3], [8], [11].

Without application of event-based PI control, the 3 N force slows the robot to a stop; i.e., the average walking rate slows from 0.50 m/s to 0 m/s.

B. Robustness to parameter mismatch

For this example, event-based PI control is used to maintain the designed average walking rate in the presence of parameter mismatch between the design model and the actual model. The actual model's torso mass, torso inertia, tibia mass and tibia inertia were set to 110 percent of the design model's values

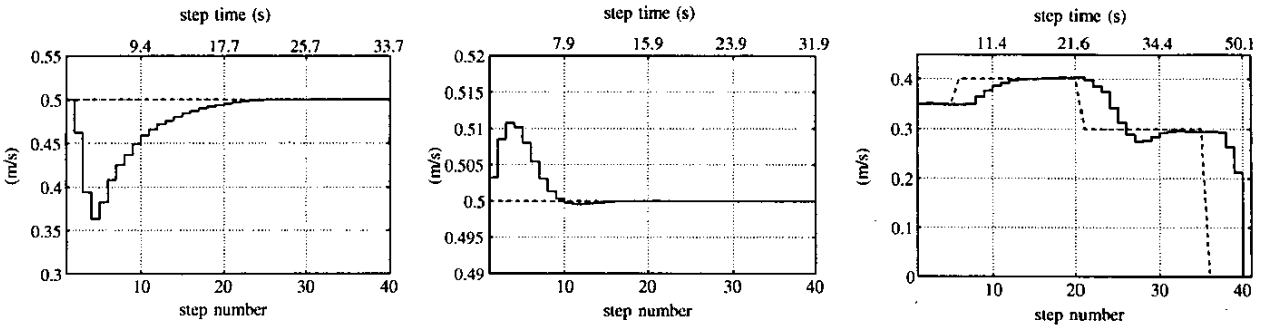

(a) Illustration of the ability of the event-based PI control to reject a disturbance force acting on the robot's hips.

(b) Illustration of the ability of the event-based PI control to maintain the designed average walking rate in the presence of parameter mismatch.

(c) Illustration of the ability of the event-based PI control to track a walking rate profile and to stop the robot on a compliant walking surface.

Fig. 2. Command (dashed) versus actual (solid) average walking rate.

while the actual model's femur mass and femur inertia were set to 90 percent of those of the design model. The robot is initialized at the fixed point of a controller whose average walking rate corresponds to 0.50 m/s. Event-based PI control with gains $K_p = 5$ and $K_I = 2$ and set-point $\eta^* = 0.5$ is applied starting on the first step. Fig. 2(b) illustrates the actual walking rate versus the commanded rate of 0.50 m/s. The peak torque for this example is 53.8 Nm, about one third of the 150 Nm possible.

Without application of event-based PI control, the parameter mismatch changes the robot's average walking rate from 0.50 m/s to 0.54 m/s.

C. Robustness to structural mismatch

This example will illustrate robustness to structural mismatch between the design model and the evaluation model. In addition, the robot will be commanded to track a walking rate profile and then slow to a stop using a single within-stride controller in conjunction with event-based PI control.

The robot model of the previous two examples is used, except that instead of assuming a rigid impact, the compliant model with dynamic friction of [8] is used. A nominal controller was designed on the basis of the rigid contact model to have an average walking rate of 0.30 m/s. When implemented on the robot with the compliant model, this yielded an average walking rate of 0.35 m/s.

In the simulation, the robot is initialized near a periodic orbit of the compliant model. Event-based PI control with gains $K_p = 0.3$ and $K_I = 0.03$ is applied starting on the sixth step with set-point $\eta^* = 0.40$. On the twenty-first step the set-point is changed to $\eta^* = 0.30$. To transition from walking to a stable standing position, on the thirty-sixth step the set-point of the event-based PI control was set to $\eta^* = 0$. Using this technique slowed the robot until it did not have enough energy to make a step, thus stopping the robot[6].

[6]The robot will, in fact, continue to rock back and forth, alternating impacts with each leg, and decreasing the kinetic energy of the robot with each impact.

The peak torque for this example is 52 Nm, about one third of the 150 Nm possible. Fig. 2(c) gives the commanded versus actual average walking rate.

ACKNOWLEDGMENTS

This work was supported by NSF grants INT-9980227 and IIS-9988695. The authors wish to thank Daniel Koditschek for insightful conversations regarding control via parameter adjustment.

REFERENCES

[1] G. Buche. ROBEA Home Page. `http://www-lag.ensieg.inpg.fr/PRC-Bipedes/English/index.php`.

[2] C. Chevallereau, G. Abba, Y. Aoustin, F. Plestan, E.R. Westervelt, C. Canduas-de Wit, and J.W. Grizzle. RABBIT: a testbed for advanced control theory. *IEEE Control Systems Magazine*, (to appear), October 2003. See [5] for a preprint.

[3] C. Chevallereau and Y. Aoustin. Optimal reference trajectories for walking and running of a biped robot. *Robotica*, 19(5):557–569, September 2001.

[4] A. Goswami. Postural stability of biped robots and the foot-rotation indicator (FRI) point. *International Journal of Robotics Research*, 18(6):523–533, June 1999.

[5] J.W. Grizzle. Jessy Grizzle's publications, 2003. `http://www.eecs.umich.edu/~grizzle/papers/robotics.html`.

[6] J.W. Grizzle, G. Abba, and F. Plestan. Asymptotically stable walking for biped robots: Analysis via systems with impulse effects. *IEEE Transactions on Automatic Control*, 46:51–64, January 2001.

[7] A. Isidori. *Nonlinear Control Systems: An Introduction*. Springer-Verlag, Berlin, third edition, 1995.

[8] F. Plestan, J.W. Grizzle, E.R. Westervelt, and G. Abba. Stable walking of a 7-dof biped robot. In *IEEE Transactions on Robotics and Automation*, 2003 (to appear). See [5] for a preprint.

[9] E.R. Westervelt and J.W. Grizzle. Design of asymptotically stable walking for a 5-link planar biped walker via optimization. In *ICRA 2002, Washington D.C.*, May 2002.

[10] E.R. Westervelt, J.W. Grizzle, and C. Canudas de Wit. Switching and PI control of walking motions of planar biped walkers. *IEEE Transactions on Automatic Control*, 48(2):308–312, February 2003.

[11] E.R. Westervelt, J.W. Grizzle, and D. Koditschek. Hybrid zero dynamics of planar biped walkers. *IEEE Transactions on Automatic Control*, 48(1):42–56, January 2003.